RESEARCH ARTICLE SUMMARY

INFLUENZA

COVID-19 pandemic interventions reshaped the global dispersal of seasonal influenza viruses

Zhiyuan Chen, Joseph L.-H. Tsui, Bernardo Gutierrez, Simon Busch Moreno, Louis du Plessis, Xiaowei Deng, Jun Cai, Sumali Bajaj, Marc A. Suchard, Oliver G. Pybus*†, Philippe Lemey*†, Moritz U. G. Kraemer*†, Hongjie Yu*†

INTRODUCTION: Despite the availability of updated seasonal influenza vaccines and treatments, annual influenza epidemics continue to cause millions of hospitalizations and substantial burden on health care systems. The global circulation of seasonal influenza lineages depends on continued virus antigenic evolution and patterns of human travel from regions with year-round transmission to temperate regions. A clearer understanding of how human influenza and other respiratory pathogens were affected by COVID-19–related restrictions will help predict how future pandemics might influence infectious diseases and help inform more effective interventions.

RATIONALE: During the COVID-19 pandemic, nonpharmaceutical interventions were introduced worldwide, which led to human behavioral changes on an unprecedented scale. This led to a decline in the global prevalence of endemic respiratory pathogens, including seasonal influenza subtypes H1N1pdm09 and H3N2 and lineages B/Victoria and B/Yamagata. The impact of changes in air travel connectivity among regions meant that the global circulation of seasonal influenza was perturbed. In this work, we assembled globally representative datasets to jointly analyze molecular, epidemiological, and international travel data to characterize how the global circulation of seasonal influenza was reshaped and when it returned to a pre-pandemic equilibrium.

RESULTS: Test positivity rates for influenza viruses dropped by >95% during the acute phase of the pandemic (April 2020 to March 2021) compared with the pre-pandemic period. We inferred that the locations where circulation of H1N1, H3N2, and B/Victoria influenza virus lineages was maintained during the acute phase were all in Asia. However, we also revealed that circulation continued in Africa, but with less influence on global circulation patterns, perhaps because of less frequent international travel. As pandemic-related restrictions weakened (albeit heterogeneously across the world), among-region virus lineage movements were detectable, and our statistical model sho strong support for association of internati air travel with between-region influenza virus movements. In the post-pandemic period (after the World Health Organization's International Health Regulations Emergency Committee declared the end of the global emergency in May 2023), the global circulation of seasonal influenza returned to pre-pandemic patterns characterized by continued viral movements and accumulation of genetic diversity—both important for maintaining transmission of seasonal influenza. The global lineage dynamics of seasonal influenza between May 2023 and March 2024 appears similar to that before the pandemic, albeit smaller in magnitude.

CONCLUSION: Our study revealed how seasonal influenza viruses are maintained during and reestablished after pandemic-related behavioral changes. The longer-term impact of the COVID-19 pandemic on influenza evolution and antigenicity will need continued monitoring through coordinated genomic surveillance and evaluation of the global transmission patterns. This is especially relevant as more regions become suitable for year-round circulation of influenza, including in Africa. ■

The list of author affiliations is available in the full article online.
*Corresponding author. Email: moritz.kraemer@biology.ox.ac.uk (M.U.G.K.); philippe.lemey@kuleuven.be (P.L.); yhj@fudan.edu.cn (H.Y.); oliver.pybus@biology.ox.ac.uk (O.G.P.)
†These authors contributed equally to this work.
Cite this article as Z. Chen *et al.*, *Science* **386**, eadq3003 (2024). DOI: 10.1126/science.adq3003

READ THE FULL ARTICLE AT
https://doi.org/10.1126/science.adq3003

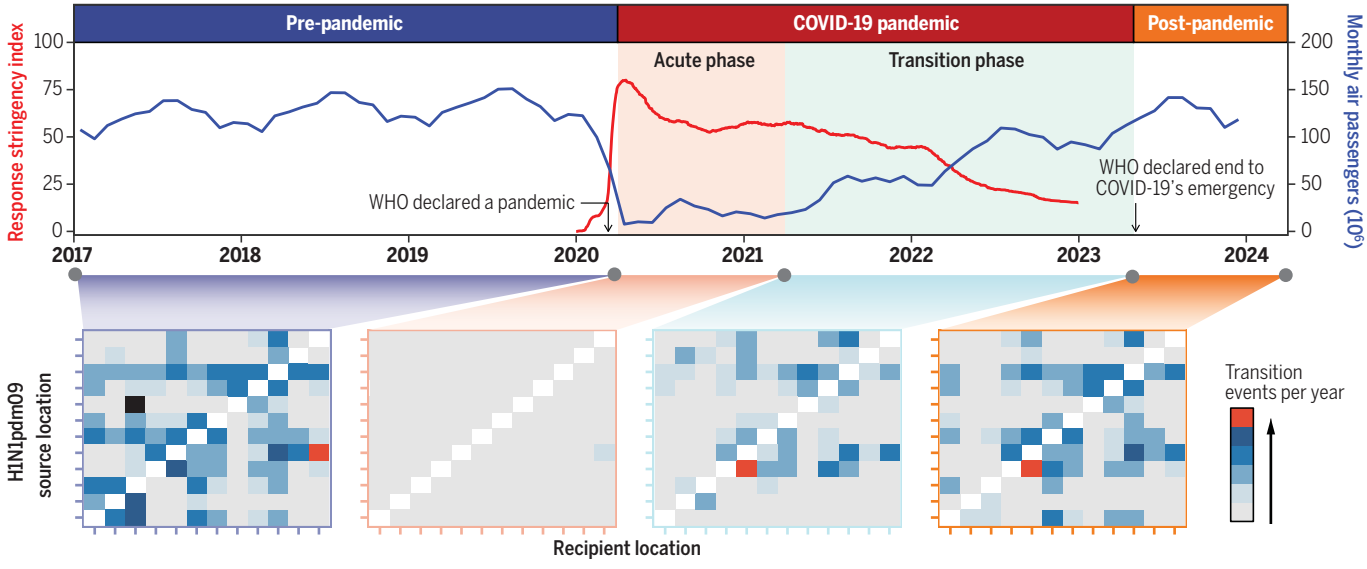

Global circulation of seasonal influenza before, during, and after COVID-19 pandemic–related restrictions. (Top) Timeline of monthly total air passenger flows (blue) and stringency of government responses averaged across all countries (red). (Bottom) Influenza lineage movement dynamics (H1N1pdm09 shown as an example) between regions during the pre-pandemic, acute pandemic, transition pandemic, and post-pandemic periods. The black box is outside the range shown in the legend.

RESEARCH ARTICLE

INFLUENZA

COVID-19 pandemic interventions reshaped the global dispersal of seasonal influenza viruses

Zhiyuan Chen[1], Joseph L.-H. Tsui[2], Bernardo Gutierrez[2,3], Simon Busch Moreno[2], Louis du Plessis[4,5], Xiaowei Deng[1,6], Jun Cai[1], Sumali Bajaj[2], Marc A. Suchard[7], Oliver G. Pybus[2,8,9]*†, Philippe Lemey[10]*†, Moritz U. G. Kraemer[2,9]*†, Hongjie Yu[1,11,12]*†

The global dynamics of seasonal influenza viruses inform the design of surveillance, intervention, and vaccination strategies. The COVID-19 pandemic provided a singular opportunity to evaluate how influenza circulation worldwide was perturbed by human behavioral changes. We combine molecular, epidemiological, and international travel data and find that the pandemic's onset led to a shift in the intensity and structure of international influenza lineage movement. During the pandemic, South Asia played an important role as a phylogenetic trunk location of influenza A viruses, whereas West Asia maintained the circulation of influenza B/Victoria. We explore drivers of influenza lineage dynamics across the pandemic period and reasons for the possible extinction of the B/Yamagata lineage. After a period of 3 years, the intensity of among-region influenza lineage movements returned to pre-pandemic levels, with the exception of B/Yamagata, after the recovery of global air traffic, highlighting the robustness of global lineage dispersal patterns to substantial perturbation.

Seasonal influenza epidemics impose a substantial burden on health care systems and cause >5 million hospitalizations of adults each year (*1*). The global dissemination dynamics of seasonal influenza are strongly associated with both global air travel (*2*–*5*) and the periodic evolution of antigenically distinct viruses that escape from vaccine- and/or infection-induced immune responses (*6*).

Changes in human behavior driven by the implementation in 2020 of nonpharmaceutical interventions (NPIs) in response to the COVID-19 pandemic (*7*) affected the evolution and circulation of seasonal influenza viruses (*8*) and other respiratory pathogens (*9*, *10*). In the wake of these NPI-associated changes in behavior and mobility, a rapid decline in influenza incidence was observed in many countries, leading to changes in the accumulation of population immunity and substantial genetic bottlenecks constraining virus diversity (*6*, *11*). Influenza transmission and dispersal resurged in late 2021 after the gradual relaxation of NPIs; however, one influenza B virus lineage, B/Yamagata, has been reported only rarely since March 2020 (*12*). This led the World Health Organization (WHO) to recommend using trivalent vaccines that exclude the B/Yamagata strain in the 2024 Southern Hemisphere and 2024–2025 Northern Hemisphere influenza seasons (*13*, *14*).

The current paradigm for influenza vaccine development emphasizes timely surveillance and evaluation of the antigenic and genetic characteristics of circulating strains (*15*), especially those sampled from previously identified source populations (including, for A/H3N2, subtropical and tropical East Asia, Southeast Asia, and occasionally India) (*16*, *17*). We sought to understand how changes in human behavior and international mobility during the COVID-19 pandemic perturbed the spatial dissemination and evolutionary dynamics of seasonal influenza lineages in a geographically heterogeneous manner.

We combined epidemiological, genetic, and international travel data in a phylodynamic framework to estimate the spatiotemporal population structure, dwell times (inferred durations between virus lineage movement events), and evolutionary diversity of seasonal influenza viruses before, during, and after the COVID-19 pandemic.

Decline in global influenza transmission

Using the key pandemic milestones (i.e., when the WHO declared the beginning and end of the COVID-19 pandemic), the COVID-19 stringency index (*18*), and air passenger volumes over time (fig. S1A), we defined three "periods" with distinct patterns of global human mobility and NPIs. Period 1 is the "pre-pandemic period," before large-scale population-level behavioral changes in response to the COVID-19 pandemic (January 2017 to March 2020). Period 2 is the "pandemic period," characterized by varying degrees of interventions that sought to limit population mixing between April 2020 and April 2023. Given the regional heterogeneities in NPIs, we divided the pandemic period into an acute phase (April 2020 to March 2021), when most countries had announced stringent restrictions on international travel, and a transition phase (April 2021 to April 2023), when international mobility recovered partially. Period 3 covers the "post-pandemic period" that started when the WHO declared the end of the COVID-19 emergency (May 2023 to March 2024).

We obtained influenza virological surveillance data from the Global Influenza Surveillance and Response System (GISRS) and supplemented them with data from national surveillance databases. GISRS collates data from specimens obtained mainly from patients with influenza-like illness and that have been tested for influenza viruses at WHO-recognized National Influenza Centres, national influenza reference laboratories, and other nonsentinel systems (*19*) (fig. S2). The antigenic and genetic characterization of influenza viruses collected through this network forms the basis of WHO annual recommendations for the composition of influenza vaccines. The number of specimens processed for influenza testing remained stable during the acute phase of the pandemic period and doubled during the transition phase (Fig. 1A). This rise is possibly due to an increase in the global capacity for virus surveillance established during the pandemic and a refocus on influenza sentinel surveillance as COVID-19 cases subsided (*20*). The proportion of laboratory-confirmed influenza cases that were subsequently sequenced during the acute phase of the pandemic was typically >10% owing to low absolute numbers of reported influenza cases; this proportion later decreased to pre-pandemic levels (Fig. 1B). Even though surveillance intensity for seasonal influenza was maintained during the pandemic, we cannot rule out possible biases in virological and genomic surveillance in the influenza databases (*19*, *21*).

The fraction of specimens that tested influenza-positive dropped significantly during the acute pandemic phase; test positivity rates (the fraction of specimens testing positive in each period) decreased by 99.2% for H1N1pdm09, 99.2% for H3N2, 96.9% for B/Victoria, and ~100% for B/Yamagata compared with the average rates during the pre-pandemic period (Fig. 1, C, E, G, and I). To account for variation among years

[1]School of Public Health, Key Laboratory of Public Health Safety, Ministry of Education, Fudan University, Shanghai, China. [2]Department of Biology, University of Oxford, Oxford, UK. [3]Colegio de Ciencias Biologicas y Ambientales, Universidad San Francisco de Quito (USFQ), Quito, Ecuador. [4]Department of Biosystems Science and Engineering, ETH Zürich, Basel, Switzerland. [5]Swiss Institute of Bioinformatics, Lausanne, Switzerland. [6]Department of Epidemiology, National Vaccine Innovation Platform, School of Public Health, Nanjing Medical University, Nanjing, China. [7]Departments of Biostatistics, Biomathematics, and Human Genetics, University of California, Los Angeles, Los Angeles, CA, USA. [8]Department of Pathobiology and Population Sciences, Royal Veterinary College, London, UK. [9]Pandemic Sciences Institute, University of Oxford, Oxford, UK. [10]Department of Microbiology, Immunology and Transplantation, Rega Institute, KU Leuven, Leuven, Belgium. [11]Shanghai Institute of Infectious Disease and Biosecurity, Fudan University, Shanghai, China. [12]Department of Infectious Diseases, Huashan Hospital, Fudan University, Shanghai, China.
***Corresponding author. Email: moritz.kraemer@biology.ox.ac.uk (M.U.G.K.); philippe.lemey@kuleuven.be (P.L.); yhj@fudan.edu.cn (H.Y.); oliver.pybus@biology.ox.ac.uk (O.G.P.)**
†These authors contributed equally to this work.

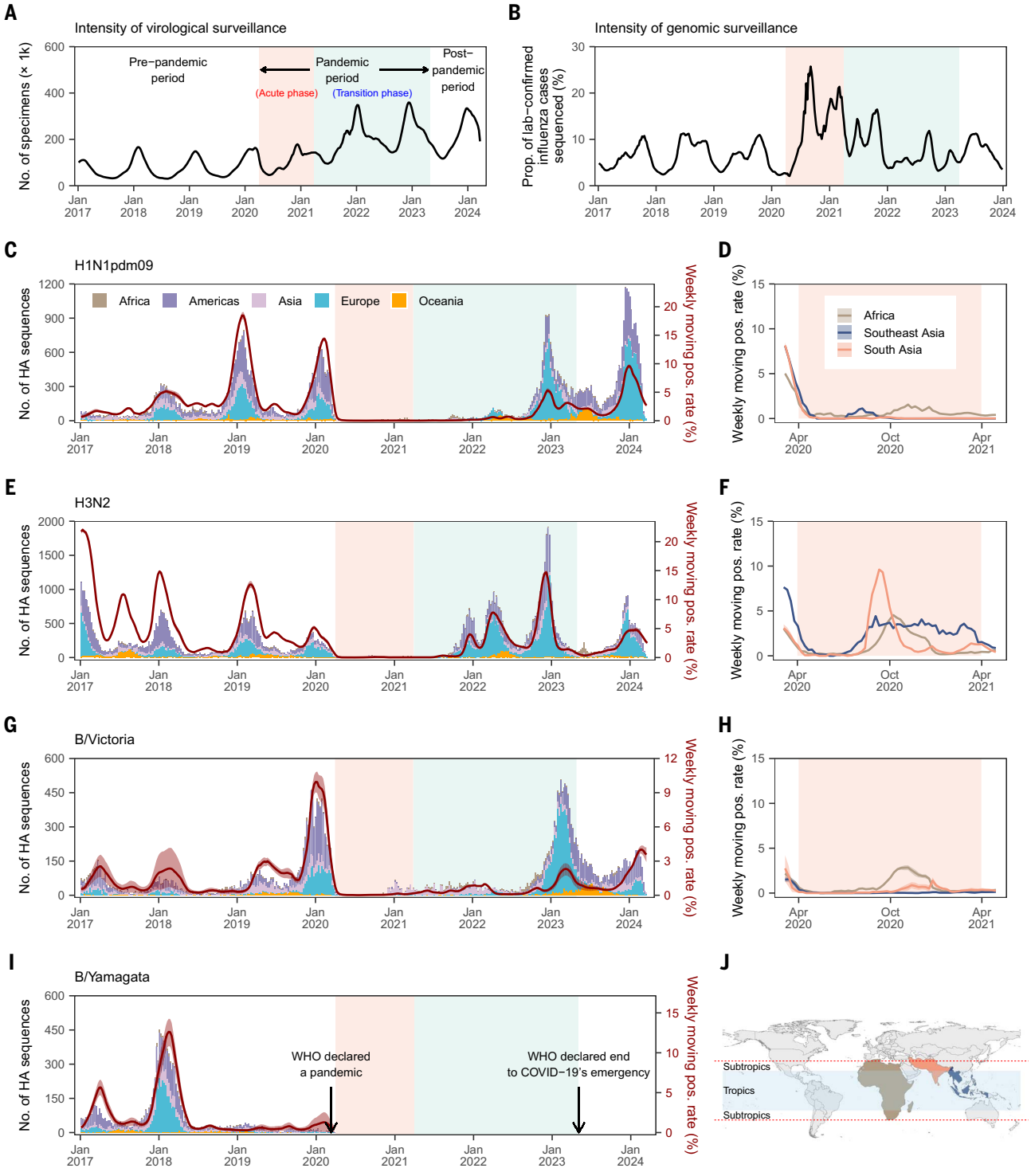

Fig. 1. Virological and genomic surveillance intensity and positivity rates of seasonal influenza viruses from January 2017 to March 2024. (**A**) Intensity of virological surveillance of influenza indicated by rolling numbers of specimens processed globally for influenza virus testing. (**B**) Intensity of genomic surveillance of influenza, as indicated by rolling percentages of reported influenza cases sequenced at high quality. (**C** to **I**) The weekly count of high-quality HA genetic sequences (stratified by continent) and global positivity (pos.) rates among tested specimens, for H1N1pdm09 (C), H3N2 (E), B/Victoria (G), and B/Yamagata (I). The positivity rates of H1N1pdm09 (D), H3N2 (F), and B/Victoria (H) are also presented separately for regions that experienced influenza waves during the acute phase of the pandemic period (Africa, Southeast Asia, and South Asia; see text). The color scheme is illustrated in (**J**). Positivity rates are presented as central-aligned rolling averages (5-week window), and the 95% intervals indicate uncertainty in inferring the specific subtypes or lineages using a Bayesian framework. The light-orange and light-blue shaded areas represent the acute and transition phases of the COVID-19 pandemic period, defined as April 2020 to March 2021 and April 2021 to April 2023, respectively.

in the number of specimens, we further calculated the ratio of positive tests to the total number of specimens processed each year (*22*), which also indicated low levels of influenza transmission after the pandemic's onset (fig. S3). Counter to these trends, several small-scale influenza outbreaks occurred during the acute pandemic phase, in Asia (mainly South and Southeast Asia) and Africa (Fig. 1, D, F, H, and J). Both areas have tropical climates that can support year-round virus circulation (*23*, *24*), and additionally, transmission could have been affected by differential responses to COVID-19 (fig. S4). After the acute pandemic phase, an H3N2 epidemic occurred during the 2021–2022 Northern Hemisphere winter with a double peak before and after the seasonal holidays, coinciding with large waves of severe acute respiratory syndrome coronavirus 2 (SARS-CoV-2) Omicron BA.1 and BA.2 infection (*25*). Subsequently, there were outbreaks of H1N1pdm09, H3N2, and B/Victoria infection during the 2022–2023 Northern Hemisphere winter (Fig. 1, C, E, and G). Substantial transmission of H1N1pdm09, H3N2, and B/Victoria resumed or continued in the post-pandemic period, but transmission of B/Yamagata did not. Only a handful of B/Yamagata cases (~20) have been reported since the onset of the pandemic, however, these might have originated from live attenuated influenza vaccines or potential data errors (*12*, *26*).

Air passenger traffic as a predictor of influenza spread

The global spatial dissemination of influenza virus was shown previously to be associated with human mobility (*2*). Disruptions to air travel, as seen in September 2001 in the United States, can affect the timing of subsequent influenza seasons (*27*). To incorporate time-specific predictors and to account for potential variation in virus dispersal rates across study periods, we constructed a four-epoch (pre-pandemic, acute pandemic, transition pandemic, and post-pandemic) Bayesian phylogeographic generalized linear model (GLM) and applied it to influenza viruses circulating from January 2017 to March 2024 (see Materials and methods). To account for potential biases in genetic sampling, we adopted three subsampling strategies for hemagglutinin (HA) gene sequences (fig. S5): (i) even subsampling, (ii) subsampling while accounting for temporal variation, and (iii) subsampling while accounting for both temporal and spatial variation (Materials and methods). These subsampling schemes were used to generate sets of ~2500 sequences for each influenza subtype or lineage, with collection dates up to the end of March 2024 (fig. S6) and sampled from 12 geographic regions (Africa, North America, South America, Europe, Russia, northern China, southern China, Japan/Korea, South Asia, West Asia, Southeast Asia, and Oceania; fig. S1B and table S1). Region definitions were based on extensive previous work on global lineage dynamics of seasonal influenza (*16*, *17*); we were able to extend previous definitions by including Africa and West Asia owing to recent increases in the availability of sequences from those locations. Covariates that describe demographic, epidemiological (i.e., influenza activity), virological, air passenger traffic, geographic, and sampling factors were included in the GLM to explore their epoch-specific associations with virus lineage movements (Materials and methods; tables S2 and S3).

As expected, during the acute pandemic phase, we observed large reductions in air passenger traffic between each pair of regions and in outbound and inbound air passenger volumes to and from each region (Fig. 2, A to D). Multidimensional scaling (MDS) analysis of among-region origin-destination (O/D) air passenger volumes (Fig. 2E) and O/D annual travel frequencies (Fig. 2F) shows that patterns of air travel during the acute pandemic phase and the first year of the transition phase diverged from pre-pandemic mobility. Among-region air travel frequencies during the second year of the transition phase were similar to pre-pandemic levels (Fig. 2F), albeit with lower absolute passenger volumes (Fig. 2E). Absolute air traffic volumes and frequency patterns recovered to pre-pandemic levels in the post-pandemic period (Fig. 2, E and F).

Although we observed changes in travel volumes and among-region frequencies, air passenger traffic remained a significant predictor of global influenza dissemination across all periods, with positive log effect sizes of 0.82 for H1N1pdm09 [95% highest posterior density (HPD) intervals = 0.71 to 0.94], 0.78 for H3N2 (95% HPD = 0.67 to 0.90), 1.06 for B/Victoria (95% HPD = 0.95 to 1.20), and 0.92 for B/Yamagata (95% HPD = 0.78 to 1.05; pre-pandemic period only) (Fig. 2G; robust to subsampling schemes: fig. S7). The activity level of influenza viruses at origin locations and antigenic distance also contributed to influenza dispersal, albeit to a smaller extent (Fig. 2G and fig. S7). The global scale of our study necessitated large-scale geographical aggregation and therefore limited our ability to include other geographically heterogeneous predictor variables. However, most of the other factors known to influence influenza transmission locally, such as humidity and demographics, are likely correlated with local influenza activity (*28*), which is included in our model. As sample size had a lower predictive power under the "even subsampling" scheme (Fig. 2G and fig. S7), we chose that sampling scheme for the main analysis, similar to previous analyses (*17*) and methodological studies that showed its robustness to sampling biases (*29*). Our results are largely robust to the spatial scale used (e.g., region versus country level), with the exception of origin population size and geographical distance (table S4). These predictors indicate that overland cross-border travel might play an additional role in the dispersal of influenza at finer spatial scales.

Reshaping global influenza circulation dynamics

We hypothesized that changes in human behavior and mobility during the pandemic perturbed the circulation dynamics of seasonal influenza lineages. To investigate this at a global scale, we used time-variable air traffic volumes as a sole predictor of among-location transition rates for each lineage and extended the phylogeographic model to include air traffic as a predictor of overall transition rates (Materials and methods). First, we estimated changes in the number of lineage movement events among regions through time (Fig. 3A) (and estimated overall lineage-specific transition rates; table S5). Second, we investigated how the among-location lineage migration network changed through time (Fig. 3, B to E, and figs. S8 and S9) and computed changes in net lineage export events (number of export events minus import events) per region per period (fig. S10). Third, we inferred the time-varying location of the trunk phylogenetic branch (fig. S11). As in previous studies, this branch can be interpreted as the lineage or lineages that successfully persist from one epidemic season to the next (*2*), under the defined sampling scheme.

The H1N1pdm09 and H3N2 lineages both exhibited seasonal fluctuations in the number of among-location movements, whereas the B/Victoria lineage showed less change through time. The number of B/Yamagata lineage movement events was low and declining in the pre-pandemic period (Fig. 3A). During the pre-pandemic period, we identified a high relative number of H1N1pdm09 lineage movements from West Asia to Africa and Europe and H3N2 and B/Victoria transitions between northern and southern China (Fig. 3, B to D). Conversely, most B/Yamagata movements at that time originated from Europe rather than Asia (Fig. 3E). Only for B/Victoria did we observe variable patterns of among-region movement intensities between seasons (fig. S8E). During the pandemic period, some B/Victoria lineage movements between northern and southern China were observed (Fig. 3D), which could be related to B/Victoria's greater ability to persist locally between seasons (*17*) and acquisition of adaptive amino acid changes observed in China during the pandemic (*30*). We applied MDS to the among-region influenza movement intensity and frequency data and found that patterns differed markedly from the pre-pandemic period (fig. S8). By 2023–2024, we inferred that among-region influenza movement intensity and frequency had largely reverted to pre-pandemic patterns (fig. S8).

Within Asia, we detected a shift in lineage net exports to South Asia for H1N1pdm09 and H3N2

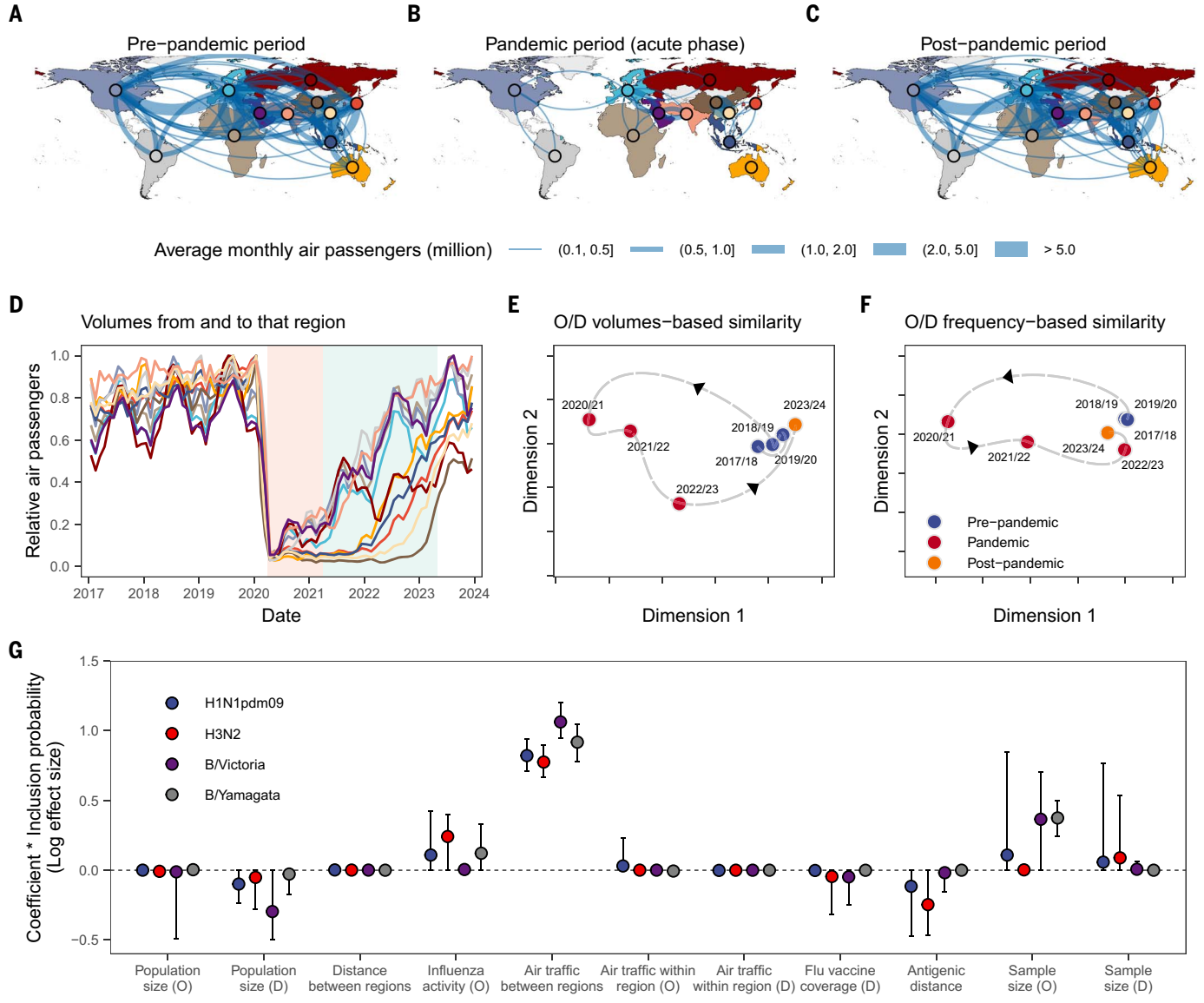

Fig. 2. Predictors of global movements of seasonal influenza virus using a four-epoch phylogeographic GLM model. (**A** to **C**) Average monthly air passenger traffic network between 12 geographic regions across the three periods. Here, only those routes with >100,000 average monthly air traffic passengers are presented, for clarity. (**D**) Relative air traffic from and to each region over time, calculated by dividing the numbers by the maximum value of each region. Air traffic between southern China and northern China was not included because we only considered between-country mobility. Colors correspond to those used in the maps in (A) to (C). (**E**) MDS visualization of the similarity of among-region origin-destination absolute air passenger volumes for different time windows. Here, each time window refers to the range from 1 April of each year to 31 March of the following year, except for 2022/2023 (April 2022 to April 2023) and 2023/2024 (May 2023 to March 2024), where the time window is aligned to the WHO's declaration of the end of the pandemic. The arc is used to show the sequence of the air passenger network. (**F**) MDS visualization of the similarity of among-region origin-destination air passenger travel frequencies for different time windows. Frequency refers to the fraction of air volume of a specific O/D journey during each time window. (**G**) Posterior summaries of the product (reported as log effect size) of the log constant-through-time predictor coefficient and the predictor inclusion probability (pooled across the time periods), for H1N1pdm09, H3N2, and B/Victoria lineages. B/Yamagata analyses were performed under a time-homogeneous (one-epoch) GLM owing to the lack of post–March 2020 gene sequences. Points and ranges represent the posterior mean and 95% HPD intervals, respectively. Location-specific predictors were included as both origin (O) and destination (D) predictors of the pairwise transition rates.

subtypes and to West Asia for the B/Victoria lineage during the pandemic period (including both acute and transition phases) (fig. S10). As air traffic inflows and outflows in West Asia recovered earlier than in Southeast Asia, we observed higher net exports of H3N2 from West Asia during the post-pandemic period (figs. S4 and S10B).

In the pre-pandemic phase, a range of plausible locations were inferred for the H1N1pdm09 trunk lineage. However, during the acute and transition pandemic phases, the H1N1pdm09 trunk location with the highest posterior probability was South Asia (fig. S11A). For H3N2, the most likely trunk location in the pre-pandemic phase was estimated to be Asia (Southeast Asia, South Asia, and West Asia) and in the acute pandemic phase was estimated to be South Asia (with a lower posterior probability for Southeast Asia; fig. S11B). South Asia, West Asia, and Africa together contributed >60% of the posterior probability for the B/Victoria trunk location during the pre-pandemic and pandemic periods, with West Asia being the most

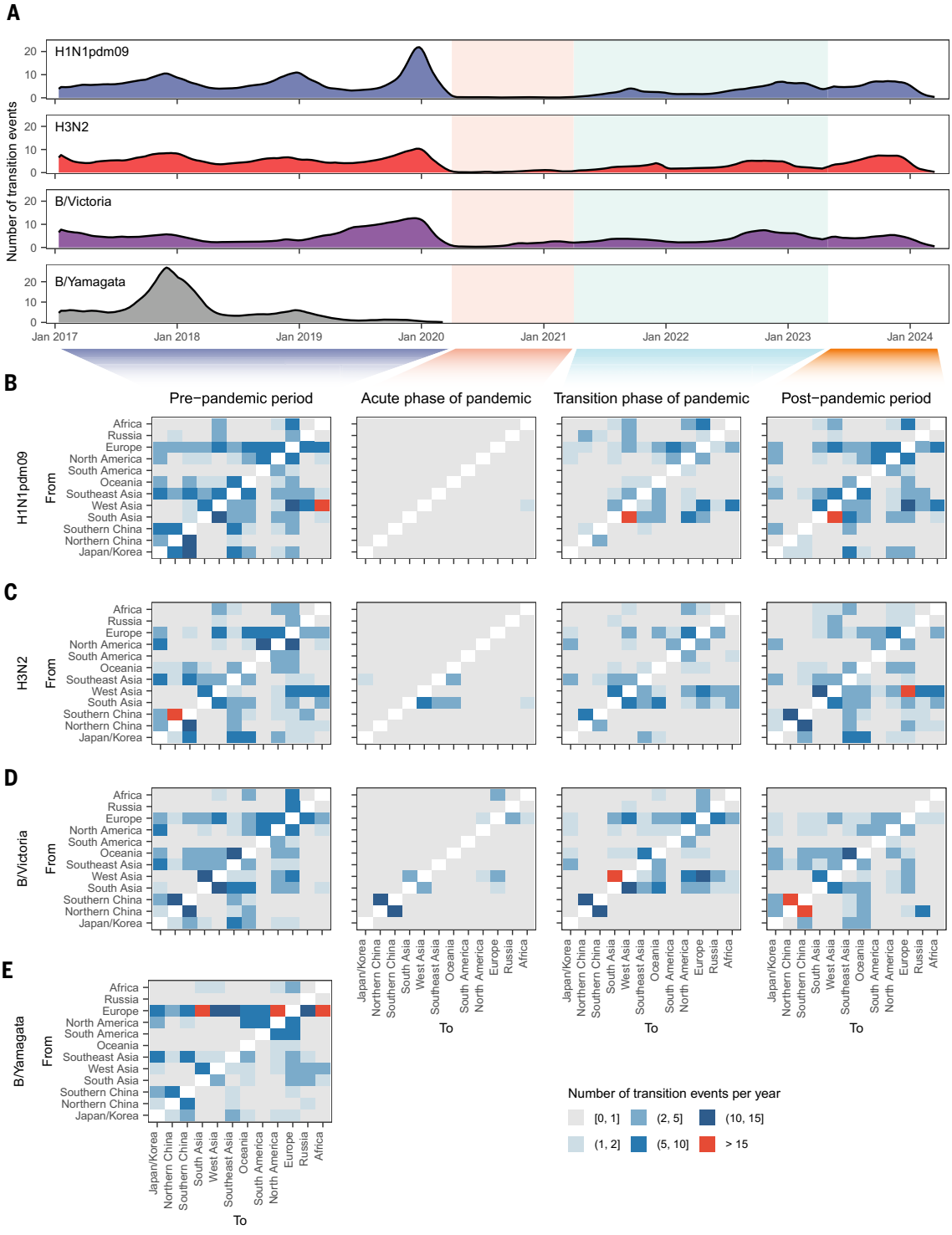

Fig. 3. Global migration dynamics of seasonal influenza virus lineages through time. (**A**) Rolling weekly Markov jump counts (location transition events) over time for the four influenza lineages. (**B** to **E**) Estimates of the number of location transition events per year between each pair of geographic regions during the pre-pandemic, acute pandemic, transition pandemic, and post-pandemic periods. Analyses are based on the posterior summaries of the Markov jumps under a time-inhomogeneous (four-epoch) GLM with only air traffic data as the predictor of overall and relative transition rates, except for B/Yamagata, which was analyzed with a time-homogeneous GLM-diffusion phylogeographic model.

likely trunk location during the acute phase of the pandemic (fig. S11C).

Heterogeneous dwell time patterns and potential correlates

Estimates of the length of time an influenza virus lineage spends in each location (dwell time) can help predict the global distribution of circulating strains and inform vaccine composition (*16*). We calculated trends in lineage-associated dwell times, which represent, for each branch present at time x, the amount of time that a lineage spends in the location inferred at time x, when moving backward through the tree (see supplementary text) (*31*).

We limited our analyses to H3N2 subtypes circulating in areas from which enough data could be obtained to estimate lineage-associated dwell times (Africa, South Asia, and Southeast Asia). We estimated that dwell times before the pandemic were generally <6 months, except for Africa in late 2019 (fig. S12A). The relatively longer dwell time of H3N2 in Africa might be attributable to the persistent circulation of the 3C.2a1b.1a clade there (fig. S13). In the acute pandemic phase, lineage-associated dwell times increased in all three regions studied, likely as a result of reduction in long-distance travel and therefore lineage movement (Fig. 3C) and strain replacement. Long dwell times were maintained

in South Asia until mid-2022, possibly as a result of its continued role as a trunk location (fig. S11B). As population mixing increased during the transition phase, international virus lineage movement and global circulation were reestablished, resulting in a drop in dwell times (fig. S12A). These results are consistent across other (tip-associated) measures of dwell time (fig. S14).

Using a Bayesian hierarchical regression model (see Materials and methods), we found that air traffic reduction (a proxy of long-distance human movement) and antigenic drift (measured using amino acid–based epitope distances over 3-, 6-, or 9-month intervals) (*32*) (fig. S15) were associated with lineage-associated dwell times of H3N2 in Africa, South Asia, and Southeast Asia (fig. S12, B and C). As reported in a pre-COVID-19 study (*17*), we found that faster antigenic drift was correlated with shorter dwell times in regions with weak seasonal forcing of influenza (fig. S12C). We also observed the converse result during the acute pandemic period in Africa: a positive association between faster antigenic drift and longer lineage-associated dwell times [z-score: 0.58, 90% highest density interval (HDI): 0.32 to 0.84] (fig. S12C). This could be a consequence of geographically structured evolution combined with limited among-location viral movement.

Temporal patterns of genetic diversity

To capture the comparative evolutionary dynamics of influenza virus lineages, we assembled a global dataset of influenza genetic sequences dating back to 2011 (see Materials and methods). As expected, the relative genetic diversity of influenza H1N1pdm09 viruses and the B/Victoria lineage declined during the acute pandemic phase and began to accumulate genetic diversity again from the beginning of the transition pandemic phase (Fig. 4B). The reduction in relative genetic diversity was slightly weaker for H3N2 viruses (Fig. 4B), as multiple clades continued to co-circulate during the pandemic period (fig. S16B).

It appears that B/Yamagata lineages stopped circulating from early 2020 onward (Figs. 1I and 4A). The relative genetic diversity of the B/Yamagata lineage began to decline in 2019 after peaking in 2018 (Fig. 4B). During 2018–2019, only one clade (Y3) of B/Yamagata lineage remained, which had been circulating since 2016 (Fig. 4A). The dominance of genetically similar Y3 viruses since 2016 is apparent as a reduction in mean pairwise diversity of B/Yamagata sequences (Fig. 4C; also apparent in dates of common ancestry, a proxy of lineage turnover; fig. S17D). Note that the evolutionary history of some influenza B virus segments is shared across the B/Victoria and B/Yamagata lineages, therefore we focused on the HA segment, which is one of three influenza B genome segments that has experienced distinct evolution (*33*).

Notably, in the HA segment of B/Yamagata, we observed a low nonsynonymous to synonymous substitution rate ratio [d_N/d_S: 0.11, 95% confidence interval (CI): 0.10 to 0.12] and no amino acid residues under positive selection, between January 2011 and March 2020, which indicates little or no detectable positive selection of the B/Yamagata HA gene (table S6) and likely corresponds to slow antigenic drift (*34*). In contrast, the B/Victoria HA segment exhibited a slightly greater d_N/d_S ratio (0.15, 95% CI: 0.14 to 0.16) and several amino acid residues under positive selection (n = 5; table S6) that are potentially immune-evasive (*30*, *35*). In contrast to HA, there are observable selective sweeps in the neuraminidase (NA) segment of B/Yamagata (table S6) (*36*), which could be linked to the repeated reassortment of NA between the B/Victoria and B/Yamagata lineages (compared with a prolonged lack of reassortment for the HA segment) (*33*). On the basis of these findings, we hypothesize that the "extinction" of B/Yamagata might be explained by a combination of susceptible host depletion (due to a large outbreak in 2017–2018), rapid human behavior changes resulting in a decline of exports from Europe at the beginning of the COVID-19 pandemic, and minimal antigenic evolution of HA (*34*, *37*). Modeling and empirical investigations are needed to assess the relative contributions of these factors to the possible disappearance of B/Yamagata.

Discussion

We found that the perturbation caused by the COVID-19 pandemic reshaped the global dissemination of seasonal influenza for 3 years, after which influenza lineage population structure returned to that observed before the pandemic. During the acute pandemic phase, influenza transmission declined globally, and lineage movements were observed in only a few regions, which typically shared tropical climatic conditions and fewer pandemic-related restrictions. Even though the intensity of global human mobility was greatly reduced during the pandemic, international travel remained the principal driver of the global dissemination of influenza lineages during the period. It has been hypothesized recently that international travel also governs the spread and mixing of other respiratory pathogens, including respiratory syncytial virus (*38*).

Further, increased global virus genomic surveillance has brought a more detailed understanding of the role of Africa and West Asia in the global circulation of influenza, which was lacking in previous phylodynamic analyses owing to data paucity (*17*). During the acute phase of the pandemic, influenza lineages tended to dwell longer in Africa than in other regions, and West Asia appeared to play an important role in the circulation and maintenance of the B/Victoria lineage. Other studies have documented the transient alteration of global population structure of H3N2 after air traffic disruption, specifically in the Asia-Pacific region during the SARS outbreak in 2003 (*2*, *17*, *39*, *40*). During that time, Southeast Asia temporarily replaced China as the H3N2 lineage trunk location (*2*, *17*, *39*). While it is possible that factors other than air traffic, demography, and geographic distance determine influenza local lineage dynamics (*28*, *41*) and onward spread, dissecting these factors at a spatiotemporal resolution higher than those presented here remains challenging within a phylodynamic framework because of the lower spatial resolution of influenza genomic surveillance (*42*). We acknowledge that other phylogeographic approaches (e.g., structured coalescent and birth-death models) may yield more mechanistic insights in the future (*43*, *44*), but such analyses are currently limited to smaller datasets and fewer geographical locations than considered here.

We observed substantial virus genetic bottlenecks during the pandemic period (*6*, *11*). The B/Yamagata lineage appears to have disappeared after the start of the COVID-19 pandemic, and the potential reasons for this are unclear (*11*, *12*). Whether B/Yamagata has gone entirely extinct, or whether it continues to persist below detection levels, is not yet resolved (*45*). Previous studies have highlighted the interplay among population size, virus mutation, and cross-immunity in predicting the circulation of seasonal influenza, in which long-range cross-immunity prevents speciation, while rapid mutation and large population sizes prevent lineage extinction (*37*). The evolutionary and circulation dynamics of seasonal influenza viruses are determined by a balance between steady decreases in population susceptibility (due to accumulating immunity against circulating strains) and the emergence of antigenically novel strains. Before the pandemic, the B/Yamagata lineage was characterized by a lower effective reproduction number (R_e) and less antigenic adaptation in the HA segment compared with B/Victoria, potentially limiting its pool of susceptible hosts (*34*, *35*). If the B/Yamagata lineage has indeed disappeared, monitoring its impact on changing infection rates of B/Victoria is critical, as some level of cross-immunity is conferred between influenza B infections (*46*).

The dwell times of seasonal influenza lineages reported in this study suggest a potential change to the level or nature of antigenic competition among existing influenza strains and the probability of emergence of geographically structured strains through regional diversification. Generally, seasons with extremely high incidence levels in the post-pandemic period might be associated with the emergence of novel clusters of influenza virus (*47*) with an increased risk of vaccine mismatch, requiring

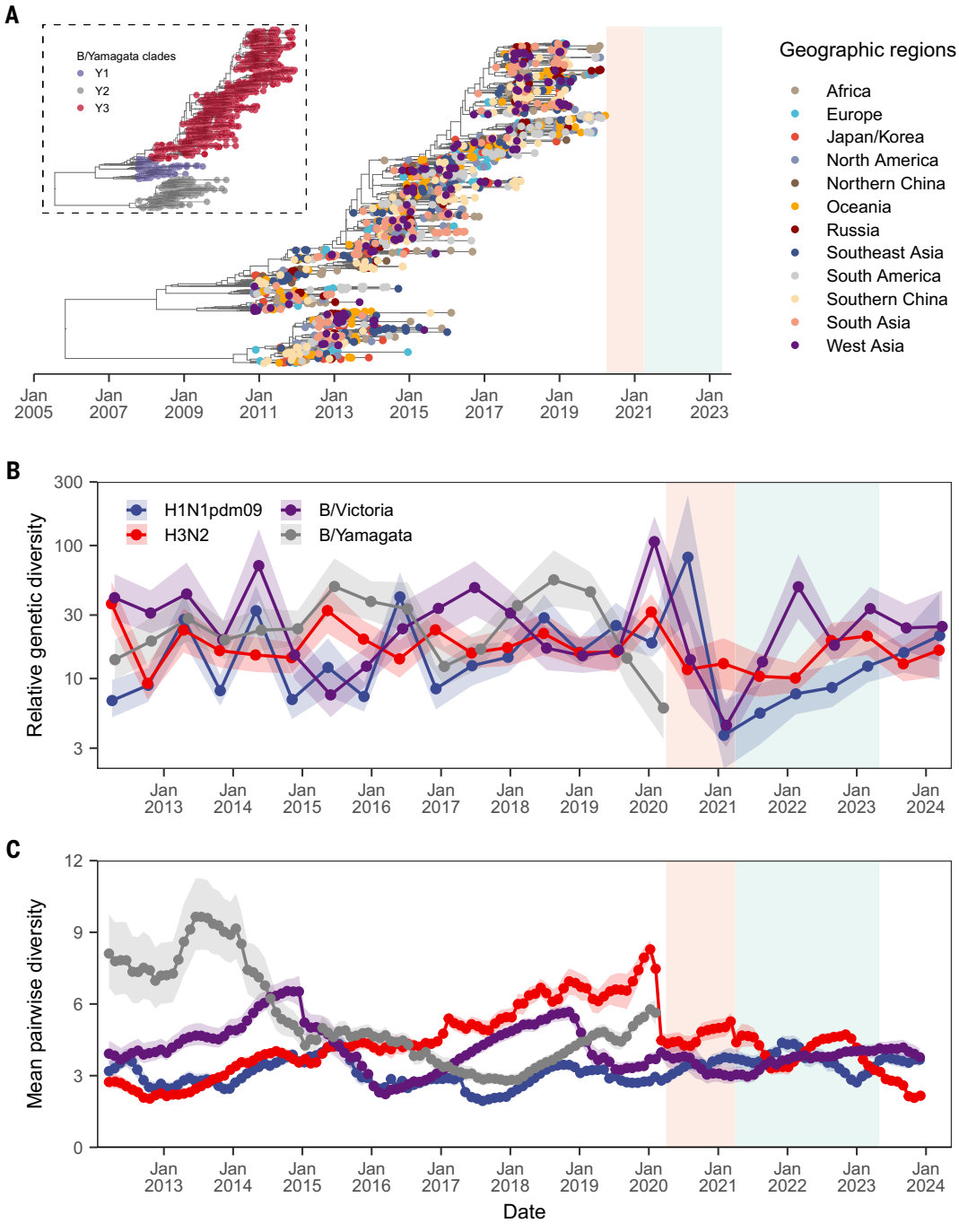

Fig. 4. Dynamics of measures of genetic diversity of seasonal influenza virus lineages. (**A**) The maximum clade credibility (MCC) tree for the B/Yamagata lineage. Tip colors represent the sampling location of each sequence. The inset shows the MCC tree with tips annotated to show the main B/Yamagata clades. (**B**) Relative genetic diversity of influenza viruses, as inferred by Bayesian Skygrid population reconstruction. (**C**) Mean pairwise diversity of influenza virus, measured as average branch length distance (patristic distance) in units of years between pairs of tips in phylogeny at monthly intervals.

enhanced surveillance. In addition to the interruption of vaccine-induced immunity owing to a drop in influenza vaccinations during the pandemic (*48*, *49*), lower accumulation of population immunity due to lack of natural infection might also lead to larger future influenza epidemics, as illustrated by the wave in Hong Kong in 2023 (*50*).

We interpret our phylodynamic results in the context of several limitations. First, as discussed elsewhere (*51*), the inferred number of virus lineage movements is not the same as the number of infected individuals, because of uneven genomic sampling and the correlated structure of phylogenetic data. To partially address potential sampling biases, we used multiple subsampled datasets, and our key conclusions are robust to this subsampling (figs. S7 and S18). Furthermore, the GISRS nonsentinel and sentinel data exhibit similar patterns, and such data appear robust when compared with wastewater monitoring data obtained from several high-income countries (fig. S19). Unfortunately, limited systematic and large-scale wastewater sampling and analysis for influenza prohibits further comparisons at present. Second, the four epochs used in our analysis are based on WHO key milestones, international air travel, and COVID-19 stringency data, and we subdivided the pandemic period into two phases (acute and transition). However, these data sources may not account for all pandemic-related NPIs nor include all local variation in NPI intensity. Reassuringly, however, our results are robust to changes in the number of epochs and their timing (figs. S20 and S21). We also included influenza positivity rates across regions as a predictor in our statistical framework to account for local intensity of influenza epidemics. Third,

the measures of lineage dwell times used here are based on phylogenetic analyses and do not equate directly to the epidemiological notion of transmission persistence across seasons, owing to the impact of phylogenetic sampling biases and uncertainty in phylogeographic inferences (*29*, *31*). Models that integrate phylogenetic analyses with detailed mathematical models of transmission of influenza could help bridge this gap in the future. Fourth, our phylodynamic analyses were constrained by the geographical resolution of available virus genome data and influenza surveillance, requiring variables to be aggregated across large geographical regions. We chose to use previously defined spatial regions to enable direct comparison with earlier studies of the global population structure of influenza (*16*, *17*). However, our results are robust to some changes in the spatial scale of analysis (e.g., country level; table S4). Future studies may benefit from higher-resolution, open, and globally representative virus genomes, combined with methodologies capable of analyzing tens of thousands of sequences.

Conclusions

The COVID-19 pandemic provided a singular opportunity to evaluate how changes in international travel patterns might perturb global influenza circulation. Our study provides an empirical evaluation of pandemic mobility restrictions on recent seasonal influenza dynamics, but the longer-term impact of the COVID-19 pandemic on influenza genetic and antigenic evolution will need continued monitoring (*8*, *52*, *53*).

Materials and methods

Data sources and preparation

Viral genetic sequence data

We downloaded all sequences of the HA segment of seasonal influenza viruses (H1N1pdm09, H3N2, B/Victoria, and B/Yamagata) publicly available in GISAID (*21*) and NCBI (GenBank) (*54*) obtained from human samples on 11 April 2024 (fig. S5). Data quality assessment, deduplication, aggregation, and cleaning steps are detailed in the supplementary text in the supplementary materials.

Influenza epidemiological surveillance data

Weekly specimens to be processed for influenza testing and notified cases of seasonal influenza at the country or territory level from January 2017 were downloaded from the FluNet tool on 11 April 2024; these data were provided by GISRS (*19*). We excluded records considered to be uninformative or nonsensible for our analysis, including weeks when no specimens were collected or when there were more positive samples than tested samples, with a total of >18,000 rows removed. Influenza epidemiological surveillance data in southern and northern China were retrieved from the weekly influenza report of the Chinese National Influenza Center, which was of higher granularity than GISRS data [see (*22*) for details]. We imputed the unsubtyped or lineage-undetermined samples into specific subtypes or lineages on the basis of the available weekly- and country-specific proportion of subtypes or lineages. To do so, we used a Bayesian model with an uninformative Beta (1, 1) prior to calculate the posterior proportions and 95% uncertainty levels, given that small tested size might cause extreme scaling.

Subsequently, we summarized the number of specimens to be processed for influenza testing over time to reflect the intensity of virological surveillance. To account for at least some of the testing heterogeneity, we estimated the positivity rates (rolling 5-week window) of each influenza subtype or lineage among all tested specimens on a weekly basis (*20*), with interval estimates determined by the 95% uncertainty levels for inferring the specific subtype or lineage. This pattern was further cross-checked with wastewater monitoring data for influenza viruses in multiple countries, including Canada, Switzerland, and Hungary (fig. S19). Intensity of genomic surveillance of influenza was indicated by the rolling percentages of reported lab-confirmed influenza cases being sequenced. To minimize the impact of heterogeneous surveillance intensity through time, we also estimated the standardized influenza activity level, calculating the ratio of positive influenza cases to the total number of specimens processed in each year (*22*).

Air traffic data

Monthly origin-destination air passenger booking data from January 2017 to December 2023 were provided by Official Airline Guide (OAG) Ltd. through a data sharing agreement (https://www.oag.com/). The data are sourced from global distribution systems (GDSs) and airlines around the world. Data harmonization and coreferencing these data against other travel and immigration datasets yield the approximate total number of air passenger bookings between pairs of airports. We refer to these data as air passenger volumes. Monthly air passenger volumes between each pair of regions were aggregated for the relevant time periods defined in fig. S1. We then used MDS to assess the network similarity using two measures (*55*): (i) vectorized among-region origin-destination (O/D) absolute air passenger volumes and (ii) frequency of among-region O/Ds in each time window. Frequency refers to the fraction of air volume of a specific O/D journey during each 1-year time window. Additionally, we computed the number of air passengers traveling within each geographic region and rescaled them (by dividing the numbers by the maximum recorded in each region). Although air traffic is only one component of overall human mobility, the temporal dynamics of air traffic within regions may still serve as a proxy for within-region long-distance human movement.

Genetic sampling and selection

Given that the phylodynamic inference is sensitive to sampling bias (*29*, *56*, *57*), we selected and subsampled genetic sequences from January 2017 to March 2024 to make their distributions as representative and even as possible while still retaining computational efficiency.

To mitigate the impact of sampling bias, we used an even sampling strategy (*29*), similar to that in (*17*). Briefly, we evenly subsampled the sequences across 12 geographic regions and years precisely defining the number of sequences to be randomly subsampled per region per year (ensuring that the total subsampled number of genetic sequences is ~2500), which reflects a relatively equitable distribution of samples across years and geographic regions for each influenza subtype or lineage (*17*).

We also adopted two additional subsampling strategies: (i) a strategy accounting for temporal variation in global influenza positivity rates and (ii) a sampling strategy accounting for spatiotemporal variation in terms of influenza positivity rates and population size across regions. In both schemes, we first determined the weekly number of sequences to be subsampled at the global level in direct proportion to the global positivity rate of each seasonal influenza virus. We then subsampled sequences evenly across 12 geographic regions for each week for the former scheme; sequences were sampled with a weight based on the product of population size and subtype- or lineage-specific influenza positivity rates per geographic region per week in the latter scheme. We retained a total of ~2500 genetic sequences for each sampling scheme to enhance comparability of our inferred transition rates. For weeks with particularly low influenza positivity rates, at least three sequences were sampled, where available, to maintain consistency in the temporal scale.

To capture evolutionary dynamics going back to 2011, we additionally adopted the even subsampling strategy (15 sequences per region per year here) to assemble a global genetic dataset of HA segments collected from January 2011 to March 2024. On the basis of that dataset, we further assembled a corresponding genetic dataset of neuraminidase (NA) segments where available.

Phylogenetic inference

Phylogenetic trees were inferred for H1N1pdm09, H3N2, B/Victoria, and B/Yamagata in a Bayesian framework using BEAST v1.10 (*58*) with the BEAGLE library v4 (*59*), in which we incorporated a starting tree (as described in the supplementary text), an HKY nucleotide substitution model with gamma-distributed among-site rate heterogeneity, a Bayesian Skygrid coalescent

prior using a Hamiltonian Monte Carlo (HMC) kernel on the population size (with grid points equidistantly spaced in 6-month intervals) (*60*), and a strict molecular clock model. Markov chain Monte Carlo (MCMC) was run for two or three independent chains, with a total of at least 160 million steps sampled every 50,000 steps for each chain. Steps were combined across chains, with the first 10 to 20% discarded as burn-in. MCMC convergence was checked in Tracer v.1.7.1 (*61*), and effective sample sizes for continuous parameters were >100. We resampled states every 300,000 to 400,000 steps, which yielded a total of ~1000 empirical trees for each influenza subtype or lineage under each subsampling strategy.

Time-inhomogeneous phylogeographic reconstruction

We used the empirical tree distributions to perform the phylogeographic reconstruction under the generalized linear model (GLM) framework (*2*). The default model assumption with constant-through-time rate of viral geographic dispersal along the phylogeny might not fit the scenario where the human behavior changes during the COVID-19 pandemic may alter the transition rate of respiratory infectious diseases. Therefore, we adopted a time-inhomogeneous GLM phylogeographic model (*31*) to allow for incorporating interval-specific predictors and accounting for the potential variation in rate of influenza dispersal before, during, and after the COVID-19 pandemic. The cutoff points that defined three periods (pre-pandemic, pandemic, and post-pandemic period) were (i) 31 March 2020, after which the global COVID-19 stringency index reached a high level, global air traffic volume drastically declined, and the WHO declared a pandemic in this month; and (ii) 30 April 2023, when global air traffic volume mostly resumed and the WHO declared an end to the COVID-19 emergency in early May 2023 (fig. S1A). To account for the regional heterogeneity of NPI implementations, we further defined two phases in the pandemic period: the acute phase, from April 2020 to March 2021, and the transition phase, from April 2021 to April 2023. Two sensitivity analyses changing the number and timing of epochs were performed: (i) three epochs using January 2022 (when restrictions regarding international travel to southern African countries were lifted) as the cutoff point to define the post-pandemic period (January 2017 to March 2020, April 2020 to January 2022, and February 2022 to March 2024); (ii) five epochs further dividing the transition phase into two epochs (January 2017 to March 2020, April 2020 to March 2021, April 2021 to March 2022, April 2022 to April 2023, and May 2023 to March 2024).

Specifically, we first adopted a four-epoch (pre-pandemic period, acute phase of the pandemic period, transition phase of the pandemic period, and post-pandemic period) GLM-diffusion phylogeographic model with interval-specific indicator variables to represent the inclusion or exclusion of predictors (*31*). Predictor inclusion was further pooled across intervals using a hierarchical model (*62*). Hierarchical and interval-specific indicators were estimated under the spike-and-slab procedure (*62*). The product of the log coefficients and the inclusion probabilities is reported as log effect sizes in our results. Here, multiple categories of potential predictors of spatial spread of influenza (e.g., population size, influenza activity, air passenger traffic, influenza vaccine coverage, antigenic distance, geographic distance, and sample sizes) were included in the GLM (table S2). The COVID-19 stringency index was not included in our analysis because it was highly correlated with within-region air traffic and only available until the end of 2022 (fig. S22). Epoch- and region-specific influenza activity was indicated by the corresponding influenza positivity rates (*20*). Owing to the limited availability of air passenger data until December 2023, the air traffic data used in the post-pandemic period only ranged from May 2023 to December 2023. Influenza vaccine coverage among elderly people was collected from a variety of sources (table S3). Antigenic distance between origin and destination regions was calculated using the Hamming distance of amino acid sequences of the HA1 region of the HA segment circulating between regions. Notably, we only adopted a time-homogeneous (one-epoch) model for B/Yamagata given the limited sequences available after the onset of the COVID-19 pandemic.

Given that air traffic between regions is able to strongly predict the spatial spread of influenza indicated by the above analyses (Fig. 2G), we subsequently specified a four-epoch GLM phylogeographic model with air traffic data as sole predictor for the relative rates and extended it to also include air traffic as a predictor for the overall transition rate scalar. Specifically, we included the asymmetric air traffic matrix between regions as the predictor for relative transition rates between each pair of regions. In addition, we incorporated the log-transformed and standardized average annual volume of air traffic in each epoch as a predictor for the overall transition rate across the four epochs. Therefore, both the relative and overall transition rates are able to vary across the four epochs, exactly rationalizing the potential impact of behavior changes during the COVID-19 pandemic on spatial transmission of influenza. To detect potential deviations in the predictive power of air mobility for relative transition rates, time-homogeneous random effects were added to the parameterization of transition rates in the model (*31*). For each influenza subtype or lineage, <10% of the transition rate random effects had a 95% HPD that excluded zero, indicating a good predictive ability. To assess the differences when only using genetic and spatial data to infer the overall transition rate, we additionally ran a model without setting up air traffic data as a predictor for the overall transition rate scalar (table S5). Five million steps were run for at least one chain and sampled every 5000 steps in the phylogeographic models.

To test the impact of spatial aggregation on the relationship between covariates and spatial dissemination of influenza viruses, we conducted a similar analysis for H3N2 at country-level resolution. Briefly, we disaggregated the 12 geographic regions into countries and chose those countries with enough genome sequences available from January 2017 to March 2024, after which a total of 106 countries (southern China and northern China were still regarded as two demes) were selected, resulting in 9857 genetic sequences subsampled using the even subsampling scheme. Running such a big dataset in a reasonable time was infeasible, and we instead used the time-calibrated starting tree as a fixed tree topology in the GLM phylogeographic analysis. Covariates in some countries (n = 18 for air traffic within the country; n = 5 for influenza activity) are not available owing to fine spatial resolution, which was alternatively replaced by the corresponding region-level value.

Bayesian hierarchical regression model

We explored the potential drivers of lineage-associated dwell time that could be estimated on a finer-grained temporal scale in the case of H3N2 subtypes circulating in Africa, South Asia, and Southeast Asia, in areas where enough data could be obtained. This question was motivated by longer lineage-associated dwell times for H3N2 in these three regions during the acute phase of COVID-19 pandemic period (fig. S12A).

Previous work indicates that local dwell times of influenza virus are associated with antigenic drift and seasonality (*17*), from which we further hypothesize that human behavior changes during the pandemic, in particular the reduction of among-region human movement (indicated by the inter-region air traffic arrivals), might influence lineage-associated dwell time as well. Here, we constructed a Bayesian hierarchical regression model to model the association of antigenic drift (w) and air traffic arrival reductions (x) with lineage-associated dwell time (y) (here measured in the units of years and changed every month) while accounting for regions and months (conceptual details presented in fig. S12B), with additional details in the supplementary materials.

REFERENCES AND NOTES

1. K. E. Lafond *et al*., Global burden of influenza-associated lower respiratory tract infections and hospitalizations among adults: A systematic review and meta-analysis. *PLOS Med.* **18**, e1003550 (2021). doi: 10.1371/journal.pmed.1003550; pmid: 33647033

2. P. Lemey *et al*., Unifying viral genetics and human transportation data to predict the global transmission dynamics of human influenza H3N2. *PLOS Pathog.* **10**, e1003932 (2014). doi: 10.1371/journal.ppat.1003932; pmid: 24586153
3. D. Brockmann, D. Helbing, The hidden geometry of complex, network-driven contagion phenomena. *Science* **342**, 1337–1342 (2013). doi: 10.1126/science.1245200; pmid: 24337289
4. L. Kakoullis *et al*., Influenza: Seasonality and travel-related considerations. *J. Travel Med.* **30**, taad102 (2023). doi: 10.1093/jtm/taad102; pmid: 37535890
5. V. Charu *et al*., Human mobility and the spatial transmission of influenza in the United States. *PLOS Comput. Biol.* **13**, e1005382 (2017). doi: 10.1371/journal.pcbi.1005382; pmid: 28187123
6. A. X. Han, S. P. J. de Jong, C. A. Russell, Co-evolution of immunity and seasonal influenza viruses. *Nat. Rev. Microbiol.* **21**, 805–817 (2023). doi: 10.1038/s41579-023-00945-8; pmid: 37532870
7. J. Zhang *et al*., Changes in contact patterns shape the dynamics of the COVID-19 outbreak in China. *Science* **368**, 1481–1486 (2020). doi: 10.1126/science.abb8001; pmid: 32350060
8. Y. Qi, J. Shaman, S. Pei, Quantifying the impact of COVID-19 nonpharmaceutical interventions on influenza transmission in the United States. *J. Infect. Dis.* **224**, 1500–1508 (2021). doi: 10.1093/infdis/jiab485; pmid: 34551108
9. J.-S. Eden *et al*., Off-season RSV epidemics in Australia after easing of COVID-19 restrictions. *Nat. Commun.* **13**, 2884 (2022). doi: 10.1038/s41467-022-30485-3; pmid: 35610217
10. S. W. Park *et al*., Predicting the impact of COVID-19 non-pharmaceutical intervention on short- and medium-term dynamics of enterovirus D68 in the US. *Epidemics* **46**, 100736 (2024). doi: 10.1016/j.epidem.2023.100736; pmid: 38118274
11. V. Dhanasekaran *et al*., Human seasonal influenza under COVID-19 and the potential consequences of influenza lineage elimination. *Nat. Commun.* **13**, 1721 (2022). doi: 10.1038/s41467-022-29402-5; pmid: 35361789
12. J. Paget, S. Caini, M. Del Riccio, W. van Waarden, A. Meijer, Has influenza B/Yamagata become extinct and what implications might this have for quadrivalent influenza vaccines? *Euro Surveill.* **27**, 2200753 (2022). doi: 10.2807/1560-7917.ES.2022.27.39.2200753; pmid: 36177871
13. World Health Organization, "Recommended composition of influenza virus vaccines for use in the 2024 southern hemisphere influenza season" (2023); https://www.who.int/news/item/29-09-2023-recommended-composition-of-influenza-virus-vaccines-for-use-in-the-2024-southern-hemisphere-influenza-season.
14. World Health Organization, "Recommendations announced for influenza vaccine composition for the 2024-2025 northern hemisphere influenza season" (2024); https://www.who.int/news/item/23-02-2024-recommendations-announced-for-influenza-vaccine-composition-for-the-2024-2025-northern-hemisphere-influenza-season.
15. World Health Organization, Global Influenza Programme (2024); https://www.who.int/teams/global-influenza-programme/vaccines.
16. C. A. Russell *et al*., The global circulation of seasonal influenza A (H3N2) viruses. *Science* **320**, 340–346 (2008). doi: 10.1126/science.1154137; pmid: 18420927
17. T. Bedford *et al*., Global circulation patterns of seasonal influenza viruses vary with antigenic drift. *Nature* **523**, 217–220 (2015). doi: 10.1038/nature14460; pmid: 26053121
18. T. Hale *et al*., A global panel database of pandemic policies (Oxford COVID-19 Government Response Tracker). *Nat. Hum. Behav.* **5**, 529–538 (2021). doi: 10.1038/s41562-021-01079-8; pmid: 33686204
19. A. J. Hay, J. W. McCauley, The WHO global influenza surveillance and response system (GISRS)—A future perspective. *Influenza Other Respir. Viruses* **12**, 551–557 (2018). doi: 10.1111/irv.12565; pmid: 29722140
20. World Health Organization, "Review of global influenza circulation, late 2019 to 2020, and the impact of the COVID-19 pandemic on influenza circulation" (2021); https://www.who.int/publications/i/item/who-wer-9625-241-264.
21. S. Elbe, G. Buckland-Merrett, Data, disease and diplomacy: GISAID's innovative contribution to global health. *Glob. Chall.* **1**, 33–46 (2017). doi: 10.1002/gch2.1018; pmid: 31565258
22. X. Deng *et al*., Regional characteristics of influenza seasonality patterns in mainland China, 2005-2017: A statistical modeling study. *Int. J. Infect. Dis.* **128**, 91–97 (2023). doi: 10.1016/j.ijid.2022.12.026; pmid: 36581188
23. L. S. Igboh *et al*., Timing of seasonal influenza epidemics for 25 countries in Africa during 2010–19: A retrospective analysis. *Lancet Glob. Health* **11**, e729–e739 (2023). doi: 10.1016/S2214-109X(23)00109-2; pmid: 37061311
24. S. Saha *et al*., Influenza seasonality and vaccination timing in tropical and subtropical areas of southern and south-eastern Asia. *Bull. World Health Organ.* **92**, 318–330 (2014). doi: 10.2471/BLT.13.124412; pmid: 24839321
25. P. Elliott *et al*., Twin peaks: The Omicron SARS-CoV-2 BA.1 and BA.2 epidemics in England. *Science* **376**, eabq4411 (2022). doi: 10.1126/science.abq4411; pmid: 35608440
26. S. Caini *et al*., Probable extinction of influenza B/Yamagata and its public health implications: A systematic literature review and assessment of global surveillance databases. *Lancet Microbe* **5**, 100851 (2024). doi: 10.1016/S2666-5247(24)00066-1; pmid: 38729197
27. J. S. Brownstein, C. J. Wolfe, K. D. Mandl, Empirical evidence for the effect of airline travel on inter-regional influenza spread in the United States. *PLOS Med.* **3**, e401 (2006). doi: 10.1371/journal.pmed.0030401; pmid: 16968115
28. B. D. Dalziel *et al*., Urbanization and humidity shape the intensity of influenza epidemics in U.S. cities. *Science* **362**, 75–79 (2018). doi: 10.1126/science.aat6030; pmid: 30287659
29. M. Layan *et al*., Impact and mitigation of sampling bias to determine viral spread: Evaluating discrete phylogeography through CTMC modeling and structured coalescent model approximations. *Virus Evol.* **9**, vead010 (2023). doi: 10.1093/ve/vead010; pmid: 36860641
30. R. Xie *et al*., Genomic epidemiology of seasonal influenza circulation in China during prolonged border closure from 2020 to 2021. *Virus Evol.* **8**, veac062 (2022). doi: 10.1093/ve/veac062; pmid: 35919872
31. P. Lemey *et al*., Untangling introductions and persistence in COVID-19 resurgence in Europe. *Nature* **595**, 713–717 (2021). doi: 10.1038/s41586-021-03754-2; pmid: 34192736
32. J. Huddleston *et al*., Integrating genotypes and phenotypes improves long-term forecasts of seasonal influenza A/H3N2 evolution. *eLife* **9**, e60067 (2020). doi: 10.7554/eLife.60067; pmid: 32876050
33. G. Dudas, T. Bedford, S. Lycett, A. Rambaut, Reassortment between influenza B lineages and the emergence of a coadapted PB1–PB2–HA gene complex. *Mol. Biol. Evol.* **32**, 162–172 (2015). doi: 10.1093/molbev/msu287; pmid: 25323575
34. K. E. Kistler, T. Bedford, An atlas of continuous adaptive evolution in endemic human viruses. *Cell Host Microbe* **31**, 1898–1909.e3 (2023). doi: 10.1016/j.chom.2023.09.012; pmid: 37883977
35. D. Vijaykrishna *et al*., The contrasting phylodynamics of human influenza B viruses. *eLife* **4**, e05055 (2015). doi: 10.7554/eLife.05055; pmid: 25594904
36. R. K. Virk *et al*., Divergent evolutionary trajectories of influenza B viruses underlie their contemporaneous epidemic activity. *Proc. Natl. Acad. Sci. U.S.A.* **117**, 619–628 (2020). doi: 10.1073/pnas.1916585116; pmid: 31843889
37. L. Yan, R. A. Neher, B. I. Shraiman, Phylodynamic theory of persistence, extinction and speciation of rapidly adapting pathogens. *eLife* **8**, e44205 (2019). doi: 10.7554/eLife.44205; pmid: 31532393
38. A. C. Langedijk *et al*., The genomic evolutionary dynamics and global circulation patterns of respiratory syncytial virus. *Nat. Commun.* **15**, 3083 (2024). doi: 10.1038/s41467-024-47118-6; pmid: 38600104
39. T. Bedford, S. Cobey, P. Beerli, M. Pascual, Global migration dynamics underlie evolution and persistence of human influenza A (H3N2). *PLOS Pathog.* **6**, e1000918 (2010). doi: 10.1371/journal.ppat.1000918; pmid: 20523898
40. International Air Transport Association (IATA), "IATA Economics' Chart of the Week: What can we learn from past pandemic episodes?" (2020); https://www.iata.org/en/iata-repository/publications/economic-reports/what-can-we-learn-from-past-pandemic-episodes/.
41. F. Guo *et al*., Ozone as an environmental driver of influenza. *Nat. Commun.* **15**, 3763 (2024). doi: 10.1038/s41467-024-48199-z; pmid: 38704386
42. Z. Chen, P. Lemey, H. Yu, Approaches and challenges to inferring the geographical source of infectious disease outbreaks using genomic data. *Lancet Microbe* **5**, e81–e92 (2024). doi: 10.1016/S2666-5247(23)00296-3; pmid: 38042165
43. N. F. Müller, D. A. Rasmussen, T. Stadler, The structured coalescent and its approximations. *Mol. Biol. Evol.* **34**, 2970–2981 (2017). doi: 10.1093/molbev/msx186; pmid: 28666382
44. A. MacPherson, S. Louca, A. McLaughlin, J. B. Joy, M. W. Pennell, Unifying phylogenetic birth–death models in epidemiology and macroevolution. *Syst. Biol.* **71**, 172–189 (2022). doi: 10.1093/sysbio/syab049; pmid: 34165577
45. M. Koutsakos, A. K. Wheatley, K. Laurie, S. J. Kent, S. Rockman, Influenza lineage extinction during the COVID-19 pandemic? *Nat. Rev. Microbiol.* **19**, 741–742 (2021). doi: 10.1038/s41579-021-00642-4; pmid: 34584246
46. Y. Liu *et al*., Cross-lineage protection by human antibodies binding the influenza B hemagglutinin. *Nat. Commun.* **10**, 324 (2019). doi: 10.1038/s41467-018-08165-y; pmid: 30659197
47. K. Koelle, S. Cobey, B. Grenfell, M. Pascual, Epochal evolution shapes the phylodynamics of interpandemic influenza A (H3N2) in humans. *Science* **314**, 1898–1903 (2006). doi: 10.1126/science.1132745; pmid: 17185596
48. S. A. Irving *et al*., Influenza vaccination coverage among persons ages six months and older in the Vaccine Safety Datalink in the 2017–18 through 2022–23 influenza seasons. *Vaccine* **41**, 7138–7146 (2023). doi: 10.1016/j.vaccine.2023.10.023; pmid: 37866991
49. H. Lymon *et al*., Declines in influenza vaccination coverage among health care personnel in acute care hospitals during the COVID-19 pandemic — United States, 2017–2023. *MMWR Morb. Mortal. Wkly. Rep.* **72**, 1244–1247 (2023). doi: 10.15585/mmwr.mm7245a6; pmid: 37943698
50. W. Xiong, B. J. Cowling, T. K. Tsang, Influenza resurgence after relaxation of public health and social measures, Hong Kong, 2023. *Emerg. Infect. Dis.* **29**, 2556–2559 (2023). doi: 10.3201/eid2912.230937; pmid: 37885047
51. J. L. Tsui *et al*., Genomic assessment of invasion dynamics of SARS-CoV-2 Omicron BA.1. *Science* **381**, 336–343 (2023). doi: 10.1126/science.adg6605; pmid: 37471538
52. E. Oliver, S. Freya, M. James, How immunity shapes the long-term dynamics of seasonal influenza. medRxiv 2023.09.08.23295244 [Preprint] (2023); https://doi.org/10.1101/2023.09.08.23295244.
53. S. P. J. de Jong *et al*., Determinants of epidemic size and the impacts of lulls in seasonal influenza virus circulation. *Nat. Commun.* **15**, 591 (2024). doi: 10.1038/s41467-023-44668-z; pmid: 38238318
54. J. R. Brister, D. Ako-Adjei, Y. Bao, O. Blinkova, NCBI Viral Genomes Resource. *Nucleic Acids Res.* **43**, D571–D577 (2015). doi: 10.1093/nar/gku1207; pmid: 25428358
55. K. V. Mardia, Some properties of classical multi-dimesional scaling. *Commun. Stat. Theory Methods* **7**, 1233–1241 (1978). doi: 10.1080/03610927808827707
56. P. Liu, Y. Song, C. Colijn, A. MacPherson, The impact of sampling bias on viral phylogeographic reconstruction. *PLOS Glob. Public Health* **2**, e0000577 (2022). doi: 10.1371/journal.pgph.0000577; pmid: 36962555
57. S. Guindon, N. De Maio, Accounting for spatial sampling patterns in Bayesian phylogeography. *Proc. Natl. Acad. Sci. U.S.A.* **118**, e2105273118 (2021). doi: 10.1073/pnas.2105273118; pmid: 34930835
58. M. A. Suchard *et al*., Bayesian phylogenetic and phylodynamic data integration using BEAST 1.10. *Virus Evol.* **4**, vey016 (2018). doi: 10.1093/ve/vey016; pmid: 29942656
59. D. L. Ayres *et al*., BEAGLE 3: Improved performance, scaling, and usability for a high-performance computing library for statistical phylogenetics. *Syst. Biol.* **68**, 1052–1061 (2019). doi: 10.1093/sysbio/syz020; pmid: 31034053
60. M. S. Gill *et al*., Improving Bayesian population dynamics inference: A coalescent-based model for multiple loci. *Mol. Biol. Evol.* **30**, 713–724 (2013). doi: 10.1093/molbev/mss265; pmid: 23180580
61. A. Rambaut, A. J. Drummond, D. Xie, G. Baele, M. A. Suchard, Posterior summarization in Bayesian phylogenetics using Tracer 1.7. *Syst. Biol.* **67**, 901–904 (2018). doi: 10.1093/sysbio/syy032; pmid: 29718447
62. G. B. Cybis, J. S. Sinsheimer, P. Lemey, M. A. Suchard, Graph hierarchies for phylogeography. *Philos. Trans. R. Soc. London Ser. B* **368**, 20120206 (2013). doi: 10.1098/rstb.2012.0206; pmid: 23382428
63. Z. Chen, M. U. G. Kraemer, Global-influenza-project-v1.0., Zenodo (2024); https://doi.org/10.5281/zenodo.13253784. doi: 10.5281/zenodo.13253784

ACKNOWLEDGMENTS

We gratefully acknowledge all data contributors, including the authors and their originating laboratories responsible for obtaining the specimens and their submitting laboratories for generating the genetic sequence and metadata and sharing through the GISAID Initiative and NCBI, on which this research is based. The acknowledgment table of genetic data used is provided in our GitHub repository (https://github.com/zychenfd/global_

influenza_project2). We thank W. Wint and J. Brittain for valuable discussions. The computations in this research were performed using the CFFF (Computing for the Future at Fudan) platform of Fudan University. **Funding:** H.Y. acknowledges financial support from the Key Program of the National Natural Science Foundation of China (82130093) and the General Program of the National Natural Science Foundation of China (82073613). M.U.G.K. acknowledges funding from The Rockefeller Foundation, Google.org, the Oxford Martin School Programmes in Pandemic Genomics (also O.G.P. and B.G.) and Digital Pandemic Preparedness, European Union's Horizon Europe programme projects MOOD (874850) and E4Warning (101086640), the John Fell Fund, a Branco Weiss Fellowship, Wellcome Trust grants 225288/Z/22/Z, 226052/Z/22/Z, and 228186/Z/23/Z, United Kingdom Research and Innovation (APP8583), and the Medical Research Foundation (MRF-RG-ICCH-2022-100069). The contents of this publication are the sole responsibility of the authors and do not necessarily reflect the views of the European Commission or the other funders. P.L. acknowledges support from the European Research Council (grant agreement no. 725422–ReservoirDOCS). P.L. and M.A.S. acknowledge support through US National Institutes of Health grant R01 AI 153044. Z.C. acknowledges financial support from the National Natural Science Foundation of China (823B2089). J.L.-H.T. is supported by a Yeotown Scholarship from New College, University of Oxford. J.C. acknowledges financial support from the Young Scientists Fund of the National Natural Science Foundation of China (82304199). **Author contributions:** M.U.G.K. and H.Y. conceived of and planned the research. Z.C., M.U.G.K., P.L., and S.B.M. analyzed the data. J.L.-H.T., B.G., L.d.P., X.D., J.C., S.B., M.A.S., O.G.P., P.L., M.U.G.K., and H.Y. advised on methodologies. Z.C. and M.U.G.K. wrote the initial manuscript draft. All authors edited, read, and approved the manuscript. **Competing interests:** H.Y. received research funding from Sanofi Pasteur, GlaxoSmithKline, Yichang HEC Changjiang, Shanghai Roche Pharmaceutical Company, and SINOVAC Biotech Ltd. None of these funds are related to this work. All other authors declare that they have no competing interests. **Data and materials availability:** Genetic sequences used were available in NCBI (https://www.ncbi.nlm.nih.gov/labs/virus/vssi/#/) with no restrictions on the use or distribution (https://www.ncbi.nlm.nih.gov/home/about/policies/) and GISAID (https://www.gisaid.org/; https://gisaid.org/terms-of-use/). Influenza virological surveillance data were available from the FluNet (https://www.who.int/tools/flunet) under terms of conditions outlined by the WHO (https://www.who.int/about/policies/publishing/data-policy/terms-and-conditions). The O/D passenger air traffic data were provided by Official Airline Guide (OAG) Ltd. (https://www.oag.com/) through a data sharing agreement and are available to replicate the analysis (*63*). Code and data to replicate the analysis are available in GitHub (https://github.com/zychenfd/global_influenza_project2) (*63*).

SUPPLEMENTARY MATERIALS

science.org/doi/10.1126/science.adq3003
Supplementary Text
Figs. S1 to S22
Tables S1 to S6
References (*64*–*81*)
MDAR Reproducibility Checklist

Submitted 9 May 2024; accepted 11 September 2024
10.1126/science.adq3003